An Isotropic Light Sensor for Measurements of Visible Actinic Flux in Clouds

J. C. H. VAN DER HAGE AND S. R. DE ROODE

Institute for Marine and Atmospheric Research, Utrecht University, Utrecht, Netherlands

(Manuscript received 15 July 1998, in final form 1 February 1999)

ABSTRACT

A low-cost isotropic light sensor is described consisting of a spherical diffuser connected to a single photodiode by a light conductor. The directional response to light is isotropic to a high degree. The small, lightweight, and rugged construction makes this instrument suitable not only for application on aircraft or under balloons but also on the ground in microclimatological studies.

A vertical profile of actinic flux in the visible range (400–750 nm) in Arctic stratus, obtained with this instrument under a tethered balloon during the FIRE experiment in 1998, is presented.

1. Introduction

Absorption or scattering of light in a cloud volume or in a volume of clear air is indifferent to the direction of the incident radiation; photons traveling upward or horizontally are absorbed alike. This cannot be said for absorption of radiation by a two-dimensional surface. The horizontal surface of the earth absorbs no upwelling or horizontal light; it can only absorb radiation with a downward component. Therefore, climatologists generally determine global shortwave radiation with an irradiance meter carefully adjusted to a horizontal position. Such a global radiation meter is not isotropic, it weighs the downward radiation with a factor $\cos\theta$, where θ is the angle of incidence on the irradiance meter relative to zenith.

For absorption studies in three-dimensional media it is better and more convenient to determine, independently of $\cos\theta$, the integrated radiance from all directions with an isotropic sensor. Such sensors are also known as ''actinic flux sensors'' or ''4π radiometers.'' Actinic flux is expressed in watts per square meter so it is in fact a flux density like irradiance; but the name ''actinic flux'' is generally accepted.

In cloud chemistry actinic flux is a basic parameter because absorbed radiation participates in photochemical reactions independently of $\cos\theta$. In polluted clouds the cloud albedo may be reduced by absorpion of light in cloud water; here again actinic flux is a more relevant parameter than global radiation. The advantages of actinic flux measurements in clouds over global radiation measurements have been discussed extensively by Madronich (1987).

The new actinic flux sensor described in this paper has the following specifications:

1) good isotropic response to radiance received from any direction (anisotropy $< \pm 5\%$),
2) perfect linear response to the integral amount of shortwave radiance received from all directions,
3) well-defined spectral response (interchangeable optical filters and photodiode),
4) fast response ($\ll$1 ms for use on aircraft),
5) lightweight construction ($<$30 g for use under balloon),
6) small dimensions (30-mm diameter for microclimatological applications),
7) output signal easy to monitor (0–1000 μA),
8) waterproof and shockproof design and easy to clean, and
9) low-cost construction and easy calibration due to isotropic and linear response.

2. Construction of the actinic flux sensor

The actinic flux sensor for visible radiation consists of a spherical diffuser that collects radiance from all directions and a light conductor that transports radiation from the center of the diffuser to a silicon diode BPW 21, which is manufactured with a fixed optical filter (see Fig. 1). The diffuser is a solid, white Delrin sphere (⌀ = 30 mm) that is supplied by a ball bearing manufacturer. The light conductor is a polished Perspex rod with flat polished ends (⌀ = 6 mm). The visible surface of the light conductor is covered with a black heat-shrink

Corresponding author address: Dr. J. C. H. van der Hage, Institute for Marine and Atmospheric Research, Utrecht University, Post Bus 80.005, 3508 TA Utrecht, Netherlands.
E-mail: J.C.H.vanderHage@phys.uu.nl

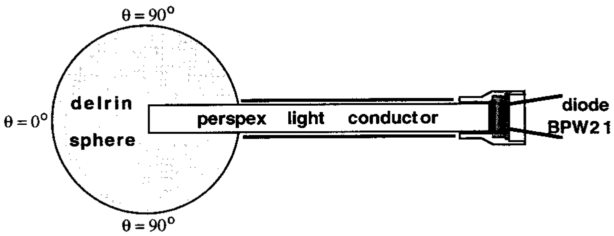

FIG. 1. Construction of actinic flux sensor.

sleeve. The mass of the instrument with a light conductor of 100-mm length is 26.2 g.

Directional sensitivities were determined on an optical bench in a collimated halogen light beam and are presented in Fig. 2, relative to the average sensitivity in the directions with $\theta = 90°$ (see Fig. 1). The light beam was wider than the sphere diameter, so the diffuser was completely illuminated. The average for every value of θ was taken from four azimuthal orientations of the sphere. The azimuthal anisotropy was less than $\pm 2\%$ for all θ values.

The main reasons why apparently identical isotropic radiation sensors have slightly different response curves (see Fig. 2) are discussed below. At the interface of the light conductor and the diffuser, mechanical demands conflict with optical demands. Optical isotropic response requires an uninterrupted layer of air between the light conductor and the diffuser. Consequently, glue is prohibited but then a mechanical joint is not realized. A compromise is found by pressing the Perspex rod into the bore of the Delrin sphere with the appropriate force. Due to the unroundedness of the bore hole and rod there will always be four small contact areas between the cylinder and the sphere where the air layer is perforated. The location of these perforations is unknown, but they produce some anisotropy that increases with the tightness of fit. Furthermore, the shape of the angular response curve depends very strongly on the penetration depth of the rod in the diffuser. The best response was found empirically for a bore hole of 14.5 mm deep in a 30-mm sphere (Fig. 2). Deeper penetration resulted in a forward sensitivity that is too high with respect to the other directions. Finally, the whiteness of the Delrin material is not quite uniform.

The actinic flux sensor has a ''blind spot'' at and around $\theta = 180°$, where the light conductor enters the spherical diffusor. At $\theta = 160°$ the response has declined to 92% of the response at $\theta = 90°$. The solid angle between 180° and 160° is given by $\omega = -2\pi(1 - \cos 160°)$ and this equals 6% of a hemisphere. Consequently, the region around the blind spot, where the response is less than 92% of the response at $\theta = 90°$, represents only 3% of the full sphere (see Fig. 2).

The spectral sensitivity of the actinic flux sensor is completely determined by the specifications of the BPW 21 photodiode. Perspex is poly(methyl methacrylate) and therefore the light conductor absorbs practically no

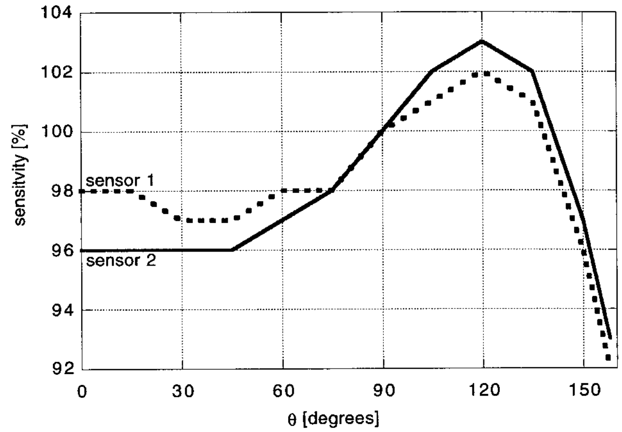

FIG. 2. Directional response of two actinic flux sensors.

light between 400 and 1200 nm (Touloukian and DeWitt 1972). Delrin is poly(oxy methylene) with a snow-white appearance. Its optical specifications could not be obtained from literature nor from the supplier. The transmission of a Delrin disk of 1-mm thickness was therefore examined in a photospectrometer. The transmission varied from 6.5% to 7.1% through the range of 400–1100 nm, so there is no selective absorption or reflection of significance by the diffuser in that range. The spectral response of the actinic flux sensor, relative to the sensitivity at 550 nm, is presented in Fig. 4.

The output current of the actinic flux sensor is for V% due to visible light (400–750 nm) and for a small fraction due to near infrared. The sensor collects downward radiation as well as upward, reflected radiation. Over a colored surface V depends on the spectral reflectivity of the surface. But over a white, gray, or black surface, V is calculated directly from

$$V = 100 \cdot \frac{\int_{400}^{750} f_{\mathrm{fig.4}} \cdot f_{\mathrm{solar}}\, d\lambda}{\int_{400}^{1200} f_{\mathrm{fig.4}} \cdot f_{\mathrm{solar}}\, d\lambda} \%. \qquad (1)$$

The function f_{solar} denotes the spectral distribution of radiant energy in daylight. For a clear-sky and a global radiation of $G = 900\ \mathrm{W\ m^{-2}}$, f_{solar} is given by Iqbal (1983) and then $V = 92\%$. Under cloudy conditions the ratio of visible and near-infrared light will be different but not dramatically so. Over an ice surface and also in clouds, more than 90% of the isotropic radiation sensor output signal must be ascribed to visible light between 400 and 750 nm.

3. Calibration of the actinic flux sensor

The calibration factor relates the output current of the photodiode to the isotropic flux density in the spectral range of 400–750 nm. A standard actinic flux sensor does not exist; therefore, the linearity of the sensor and

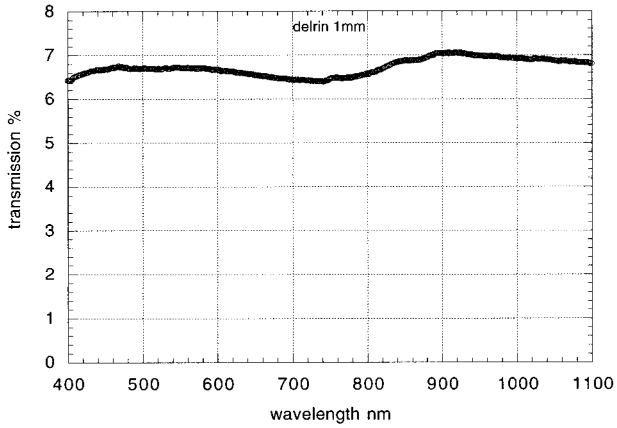

FIG. 3. Spectral transmission of a Delrin plate, 1 mm thick.

the sensitivity for the visible part of solar radiation was tested by a comparison with the Royal Netherlands Meteorological Office version of the monochromatic radiative transfer model TUV (Madronich 1998). We used 60 wavelengths between 400 and 740 nm and a nonequidistant wavelength interval. The ground albedo in the model was 0.85, which is a typical value for clean snow (Kondratyev 1969) corresponding to the albedo measured at the experimental site. For a clear sky, Rayleigh scattering is the principal mechanism that determines the spectral distribution of the downward direct and diffuse component of the actinic flux in the visible light band. Since Rayleigh scattering depends on the wavelength and the optical thickness of the atmosphere, the spectral distribution of the downward component of the actinic flux is dependent on the solar zenith angle. With the model we calculated the total actinic flux (F_{tot}) between 400 and 750 nm for different zenith angles between 55° and 80°, which are representative values for the Arctic region where the measurements were made. Finally, the spectral distribution of the calculated actinic flux was weighted ($F_{weighted}$) with the spectral

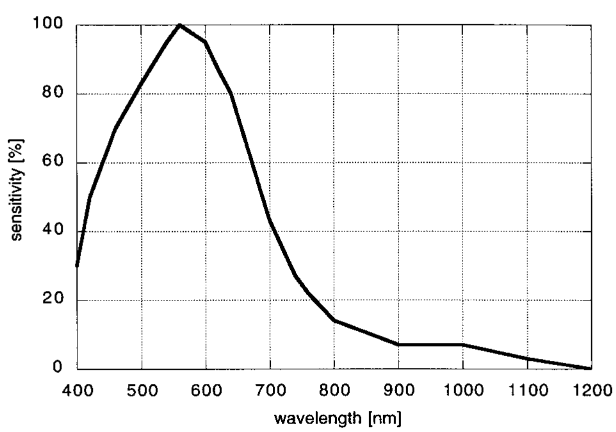

FIG. 4. Relative spectral response of actinic flux sensor with BPW 21 photodiode.

TABLE 1. Clear-sky calibration factors for the balloon actinic flux sensor. Here F_{vis} represents the actinic flux in the visible light band between 400 and 750 nm, while F_{550} is the corresponding monochromatic actinic flux at 550 nm.

F_{vis}	F_{550}	Sensor output
7.45 W m^{-2}	0.0232 W m^{-2} nm^{-1}	1.00 μA ± 5%

response function $f_{fig.4}$, according to Fig. 4. After comparing $F_{weighted}$ with the sensor output we conclude that the response of the instrument is linear within 0.5%. A similar comparison was performed for a cloudy atmosphere, and we found that the linearity of the instrument was not affected by clouds.

For the final calibration of the actinic flux sensor we used the model results and compared these with measurements made during a day with clear skies. For this purpose we used data collected on 24 May 1998; on this day a radar, a ceilometer, and a lidar, which were all operational at the same site, did not detect any clouds. Table 1 is a summary of the calibration factors, including a factor that gives the monochromatic actinic flux F_{550} at 550 nm.

4. Application of the actinic flux sensor in Arctic clouds during the FIRE III experiment

In April and May 1998 some 50 ascents were made with the actinic flux sensor suspended under a 12 m^3 tethered balloon from the frozen surface of the Beaufort Sea (76°N, 165°W) during the First ISCCP Regional experiment/Surface Heat Balance of the Arctic Ocean (FIRE III/SHEBA) measurement campaign. The instrument was connected to a meteorological balloon radio transmitter with 9 m of thin cable. Due to this length of cable the balloon would never shield more than 1% of the sky from the sensor. By definition a perfect isotropic sensor need not be oriented in any specific direction. This is a great practical advantage of isotropic sensors over irradiance sensors, especially in balloon measurements. However, the present sensor is not perfect; it has a blind spot where the light conductor enters the spherical diffusor (see Fig. 2). But the orientation of the sensor under the balloon is such that this blind spot looks upward, coinciding with the small solid angle that is already shielded by the balloon itself. Therefore, from all possible directions only the small (about 1%) fraction around zenith is shielded for the isotropic sensor. With low elevations of the sun the zenith represents a relatively dark part of the sky; and so only a negligible fraction (<1%) of the total radiance is erroneously ignored through shielding errors.

A vertical sounding of the actinic flux registered in an Arctic stratus cloud is presented in Fig. 5. This sounding, taken on 8 May around 1700 local solar time, shows all the typical aspects of a profile expected in a stratus cloud at low solar elevation over an ice surface. Figure 5 is a perfect illustration of the Madronich (1987) trans-

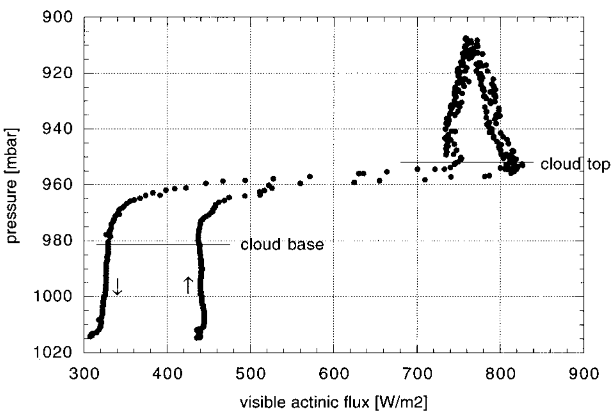

FIG. 5. Actinic flux profile through Arctic stratus. The arrows indicate, respectively, the descent and the ascent of the balloon.

fer model for radiation in clouds. Note that the profile has two branches: one for the ascent and the other for the descent through the cloud. These branches do not coincide because the solar elevation changed during this sounding, which took 80 min. Under the cloud there was no direct radiation and the total actinic flux F is related to the global diffuse radiation G_{dif} according to Madronich (1987) as

$$F = 2G_{\mathrm{dif}}(1 + \alpha). \quad (2)$$

From data given by Iqbal (1983) we find, at sea level, that 1 W m^{-2} of shortwave irradiance contains 0.495 W m^{-2} of visible irradiance (400–750 nm). Consequently, under a cloud in the absence of direct radiation

$$F_{\mathrm{vis}} = 0.99G_{\mathrm{dif}}(1 + \alpha). \quad (3)$$

And indeed, the ratio of visible actinic flux under the cloud at the beginning and end of the sounding from 440 to 310 W m^{-2} is within 1.5% of the ratio of the observed global radiation, which decreased from 223 to 156 W m^{-2} during the same period.

The cloud top is indicated very distinctly, but the famous theoretical peak value in the actinic flux just below cloud top is not visible in Fig. 5. This peak value is associated with an enhancement factor 2 $\cos\theta_o$, operating when collimated sunlight is transformed to diffuse light (Madronich 1987). However, θ_o was 72° during this sounding and as $\cos 72° = 0.31$, the enhancement factor was now less than unity (0.62). In the Arctic regions θ_o is always larger than 43.5° and consequently, the ''Madronich peak'' in the actinic flux just below cloud top will rarely be observed there.

The cloud base is not indicated by any flux gradient at all because the optical properties of the ice floor resemble those of a cloud surface very closely. This optical resemblance also explains why on other afternoons, in the absence of clouds the actinic flux at ground level reached similar values as the present actinic flux found above cloud in Fig. 5.

The sensor may collect water droplets and ice in the cloud. The effect of water droplets was checked in the laboratory by spraying the diffuser with small droplets from a nebulizer. The droplets had no measurable effect on the isotropy nor on the sensitivity of the actinometer. The effect of ice has not been studied yet. During some balloon ascents the sensor collected a thick crust of rime that was usually deposited asymmetrically on one side of the diffuser sphere. The sounding presented in Fig. 5 was free of rime.

Acknowledgments. The investigations were in part supported by the Netherlands Geoscience Foundation with financial aid (Grant 750.295.03A) from the Netherlands Organization for Scientific Research. The authors are indebted to W. Boot for his technical assistance.

REFERENCES

Iqbal, M., 1983: *An Introduction to Solar Radiation.* Academic Press, 390 pp.

Kondratyev, K. Ya., 1969: *Radiation in the Atmosphere.* Academic Press, 912 pp.

Madronich, S., 1987: Photodissociation in the atmosphere. Part 1: Actinic flux and the effects of ground reflections and clouds. *J. Geophys. Res.,* **92,** 9740–9752.

——, cited 1998: TUV software package. [Available via anonymous ftp: ftp://sasha.acd.ucar.edu.]

Touloukian, Y. S., and D. P. DeWitt, 1972: *Thermal Radiative Properties.* Vol. 8. Plenum, 1763 pp.